Single-Frequency 336 W Spliceless All-Fiber Amplifier Based on a Chirally-Coupled-Core Fiber for the Next Generation of Gravitational Wave Detectors

Sven Hochheim, Eike Brockmüller, Peter Wessels, Joona Koponen, Tyson Lowder, Steffen Novotny, Benno Willke, Jörg Neumann, and Dietmar Kracht

***Abstract*—Specialty fibers such as chirally-coupled-core fibers show a high potential for further power scaling of single-frequency fiber amplifiers. For the first time, we demonstrate a spliceless all-fiber amplifier, where all optical components are directly integrated in a single Yb^{3+}-doped 3C-fiber. Such a spliceless laser design enables a compact and robust architecture using specialty fibers, while maintaining excellent beam properties. At an output power of 336 W operating at 1064 nm, a fundamental mode content of 90.4% at a polarization extinction ratio above 13 dB was measured without any impact of transverse mode instabilities or other parasitic effects. This work emphasizes the field of applications of 3C-fibers in high-power laser systems.**

***Index Terms*—Chirally-coupled-core fiber, gravitational wave detector, signal and pump combiner.**

I. Introduction

In THE recent decade, all-fiber lasers or amplifiers satisfied the demand for compact and robust laser architectures. Such systems are robust and maintenance-free and exhibit frequently a simple plug and play operation. Compared to free-space designs, fiber lasers enable a high-power optical output level while maintaining beam quality on a compact footprint. The advantage of compact designs compared to free space architectures is applied in almost all optical applications. It is therefore not surprising that for the challenging laser systems of gravitational wave detectors (GWD), fiber-based systems are also considered as a suitable option for a new generation of the observatories.

Single-frequency lasers such as those developed at the 200 W-level for advanced LIGO use solid-state injection-locked Nd:YAG ring oscillators to achieve the required optical output power [1]. Current developments of Nd:YVO_4 high-power master oscillator power amplifier laser system also show excellent results [2]. These laser systems fulfill the special requirements of GWDs regarding power and noise specifications. However, the optical output power level of such systems has to be increased significantly for an improved sensitivity in future detector architectures [3]. Current solid-state laser designs only achieve more than several hundreds of watts at the expense of usability, maintenance procedures and system complexity. At increased output power levels, solid-state lasers require complex cooling strategies and an improved thermal lensing management with a tendency to instabilities and reduction of beam quality [4]. However, laser systems used for GWDs must maintain the specifications in continuous 24/7-operation. Therefore, compact and robust laser or amplifier designs are required without long maintenance procedures.

Fiber and fiber-based component technology can be a suitable alternative to overcome these limitations [5]. In the recent decade, several single-frequency fiber amplifiers have been developed and demonstrated further power scalability of such devices. In 2008 Mermelstein *et al.* presented 194 W output power [6], Zhu *et al.* demonstrated up to 511 W output power [7] and in 2014 Pulford *et al.* presented an output power level of 811 W [8]. In addition to a very high output power level fiber amplifiers also enable to fulfill GWD requirements regarding low noise levels and exceptional beam quality with a fundamental mode content above 90% [5]. Besides, a sufficient heat distribution is supported by the fundamental properties of the fibers, which allow for compact fiber amplifiers with simple operation and maintenance. In this regard, Wellmann *et al.* achieved recently 200 W in an engineering all-fiber system [9]. Additionally, Dixneuf *et al.* demonstrated 365 W of low noise optical power [10].

Manuscript received June 7, 2021; revised October 15, 2021; accepted December 5, 2021. Date of publication December 10, 2021; date of current version April 4, 2022. This work was supported in part by the Max-Planck-Institute for Gravitational Physics, Hanover, Germany, and in part by the Deutsche Forschungsgemeinschaft, DFG, German Research Foundation, under Germany's Excellence Strategy - EXC 2123 QuantumFrontiers under Grant 390837967. *(Corresponding author: Sven Hochheim.)*

Sven Hochheim, Eike Brockmüller, Peter Wessels, and Dietmar Kracht are with the Laser Development Department, Laser Zentrum, 30419, Hannover, Germany, and also with the Cluster of Excellence Quantum Frontiers, 30167 Hannover, Germany (e-mail: s.hochheim@lzh.de; e.brockmueller@lzh.de; p.wessels@lzh.de; d.kracht@lzh.de).

Joona Koponen and Steffen Novotny are with the nLight Oy, 08500 Lohja, Finland (e-mail: joona.koponen@nlight.net; steffen.novotny@nlight.net).

Tyson Lowder is with the nLIGHT Inc., Vancouver, WA 98665 USA (e-mail: tyson.lowder@nlight.net).

Benno Willke is with the Max -Planck-Institut für Gravitationsphysik (Albert-Einstein-Institut), Leibniz Universität, 30167 Hannover, Germany (e-mail: benno.willke@aei.mpg.de).

Jörg Neumann is with the Laser Development Department, Laser Zentrum, 30419, Hannover, Germany (e-mail: j.neumann@lzh.de).

Color versions of one or more figures in this article are available at https://doi.org/10.1109/JLT.2021.3133814.

Digital Object Identifier 10.1109/JLT.2021.3133814

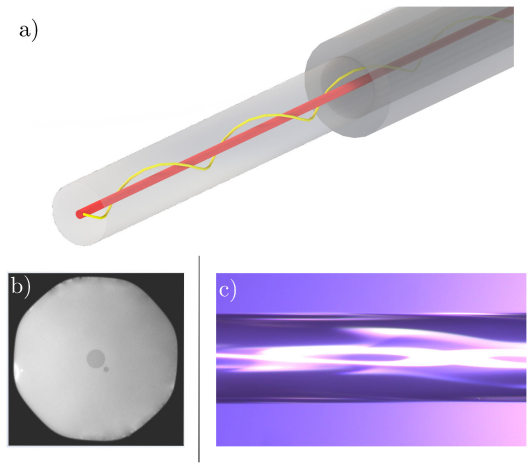

Fig. 1. (a) Illustration of the 3C-fiber with one satellite core. (b) Cross-section of an Yb700-34/250DC-3 C fiber. (c) Microscopic side view of the 3C-fiber.

Scaling single-frequency fiber laser sources to power levels sought by GWD is hampered primarily by stimulated Brillouin scattering (SBS). To avoid this and other nonlinear optical effects, fibers of larger core compared to traditional single-mode fibers are used and specialty fiber designs including photonic crystal and photonic bandgap fibers (PCF and PBG [11], [12]) have been developed and successfully tested, which are able to retain single mode operation in such larger-core fibers. In conjunction with these developments, the particular fiber concept of a chirally-coupled-core (3C) fiber has been specifically designed with a large mode area core [13]. To ensure a single-mode operation, the signal core is additionally chirally surrounded by one or more satellite cores (see Fig. 1). The higher order modes (HOM) experience high losses in the signal core, because of quasi-phase matching and the helical geometry [14]. The principal performance of 3C-fibers in single-frequency all-fiber amplifiers has already been proven [15]. The all-solid design of the 3C-fiber allows for the manufacturing of optical components with this fiber type without any impact on the fiber structure while maintaining fiber properties and beam quality. For that purpose we designed highly-integrated optical components such as signal and pump combiner combining up to 4 fiber-coupled multi-mode pump sources using side-pumping technology or cladding light stripper in 3C-fibers. These components enable compact and robust all-fiber laser systems, which can also be implemented in almost any fiber laser or amplifier. Using these components, the setup of a spliceless all-fiber amplifier based on a single 3C-fiber will be described in the following.

II. Setup of the MOPA System

Our fiber laser source exhibits a master-oscillator/power-amplifier architecture (MOPA) with the fiber amplifier portion of it characterized by a two-stage (pre- and main-amplifier) design, as shown in Fig. 2. For this purpose a single-frequency non-planar ring oscillator (NPRO, *Innolight* Mephisto 2000NE) with a narrow laser linewidth ($<$1 kHz over 100 ms) was used as master oscillator. The particular NPRO seed source technology has proven low frequency- and intensity-noise properties at a continuous-wave output power of 2 W at 1064 nm. An optical isolator protects the seed source from back-reflections and optics are in place to mode-match the laser beam into a standard PM-step-index fiber of the pre-amplifier, so that 1.4 W are guided within the fiber core.

The pre-amplifier was based on a single piece of a 3 m long 10/125 μm Ytterbium (Yb^{3+})-doped PM-fiber (Yb1200-10/125DC-PM, *nLight*) and was operated in counter-propagating configuration. An in-house made cladding light stripper (CLS) was used to remove any residual light of the cladding and was directly integrated in the Yb^{3+}-doped fiber. The CLS was based on a micro-structured cladding produced with a CO_2-laser and enabled a cladding light suppression of typically 20 dB [16]. Instead of the most common type of fiber combiner, which is based on the fiber end face pumping technique, the pump combiner was designed using a side-pumping technology [17]. Here, the light of two fiber-coupled pump diodes (BMU30-975-01-R/R02, *II-VI*) with a maximum output power of 30 W each at 976 nm was coupled via tapered pump fibers fused to the side of the active signal fiber with a coupling efficiency of more than 90%. The seed signal was amplified by this pre-amplifier up to a power level of 15 W with a slope efficiency of 78% referred to the absorbed pump power.

The interface between the pre- and main-amplifier was a home-made compact Faraday isolator with robust fiber interfaces to protect the system from backward propagating light with the 10/125 μm Yb^{3+}-doped fiber from the pre-amplifier as input- and a 3C-fiber as output fiber. AR-coated fiber end caps were used as high-power connector interfaces to the isolator and were directly fused to the fibers using a CO_2-laser. On the one hand, the end caps protected the fiber end facets mechanically and on the other hand they do not degrade the beam quality. This plug-in design allowed for an easy replacement of the main-amplifier and an integration of almost any other amplifier architecture. Additionally, the isolator had an extra monitor port based on a polarization beam splitter to measure the performance of the pre-amplifier. For the minimization of the excitation of higher order transversal modes, the 3C-fiber was tapered similar to a mode field adapter, cleaved at the taper waist and spliced to the end cap. Therefore, the input- and output-fiber of the isolator had the same mode field area so that a 1-to-1 imaging of the beam within the isolator could be realized. The short tapered area of the 3C-fiber did not show any effect of a degradation of beam quality, even if the filter effect of the side cores was minimized in this area. This architecture combines the advantages of two optical fiber components: a fiber-based isolator and a mode field adapter using specialty fibers. Finally, measured parameters of the isolator of an internal loss of $<$1.5 dB and an isolation of $<$25 dB were determined.

The main-amplifier module consisted of a 3 m Yb^{3+}-doped 3C-fiber with a core diameter of 34 μm (Yb700-34/250DC-3 C, *nLight*). As in the pre-amplifier, all necessary optical components were directly integrated into the 3C-fiber to ensure an optimal beam quality without additional losses due to splices. The key component of such an amplifier system was the high-power signal and pump combiner operating in counter-propagating configuration. The all-solid fiber structure of the 3C-fiber enabled the fabrication of these components. Using

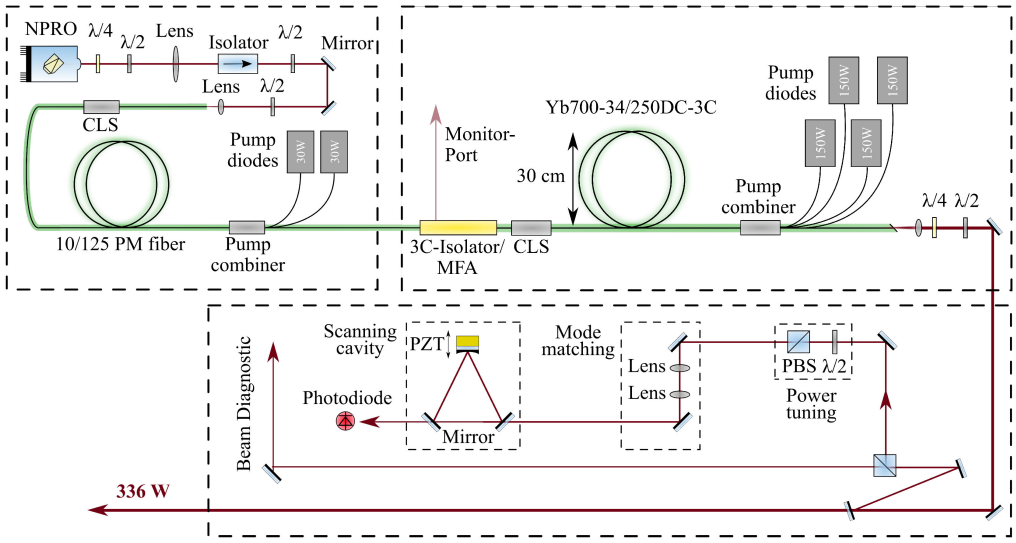

Fig. 2. Experimental setup of the monolithic amplifier based on a 3C-fiber in the second amplifier stage. The system consists of a non-planar ring oscillator as seed source, a pre-amplifier designed with a single piece of a standard Yb^{3+}-doped fiber and a main-amplifier manufactured with a single piece of an Yb^{3+}-doped 3C-fiber.

the side-pumping technique the pump light was coupled via the outermost cladding surface into the 3C-fiber with a pump light coupling efficiency of >70%. Further details on the loss mechanism and cooling requirements are described in detail in Ref. [18]. The key advantage of this technology was the uninterrupted helical structure and the elimination of the need for an additional fusion splice in conjunction with signal mode matching. Four fiber coupled pump diodes with an optical output power of 150 W each at 976 nm were spliced with a matched core diameter of 106.5 μm to the input pump fibers of the pump combiner. The counter-propagating pump configuration has the double advantage of reducing the effective interaction length for nonlinear optical parasitic effects (by inducing a near-exponential power growth along the fiber with most amplification occurring near the output end) and establishing a thermal gradient, both of which increase the SBS threshold power compared to co-propagating pumping [19].

The residual light in the cladding of the 3C-fiber was suppressed by a further in-house made CLS. The CLS was directly integrated into the 3C-fiber and achieved a similar suppression of 19 dB, such as a CLS integrated in standard fibers [16]. The grooves in the 3C-fiber produced by a CO_2-laser are shown in Fig. 3. In the manufacturing process the grooves were generated on different sides in the fiber to achieve an optimal suppression of propagating light.

In previous experiments, Stock *et al.* demonstrated a 3C-fiber amplifier with high peak power of multiple kW, which showed effects of nonlinear polarization instabilities [20]. Please note, that the 3C-fiber is a non-PM fiber without additional stress rods. For suppression of polarization effects and a conservation of the polarization stability also in the low power regime, the method of injecting circularly polarized seed light was used in our previous amplifier system [14], [15], [20]. Further research studies also show a stable performance at a linear polarization [21]. Therefore, the linearly polarized light was converted in the 3C-fiber isolator via a half and quarter wave plate into a polarization state

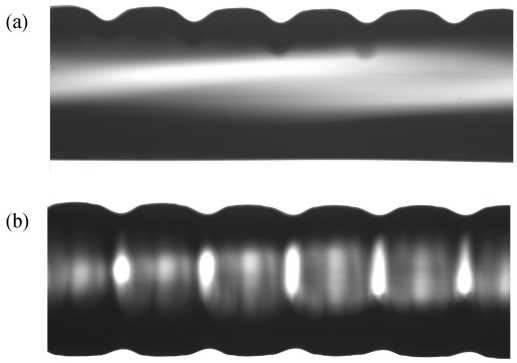

Fig. 3. Images of the manufactured cladding light strippers with grooves on a single side in (a) and on three sides in (b) with a suppression of propagating cladding light of 19 dB.

such that the best possible and stable PER was achieved after the amplifier system. The impact of the behavior of different polarization states propagating through the 3C-fiber are part of more extensive studies and are beyond the scope of this work. After the amplifier, the polarization state was converted back into a linearly-polarized beam.

The 3C-fiber has a nominal absorption of 2.15 dB/m at 920 nm and has been coiled on an aluminum spool with 30 cm diameter for thermal management. The spool was in thermal contact with a passively water-cooled heatsink. The output facet of the 3C-fiber has been angle cleaved to avoid back reflections into the amplifier system.

III. Characterization of the 3C-Fiber Amplifier System

A. Optical Output Power

The measured optical amplifier output power versus the pump power is shown in Fig. 4(a). With an absorbed pump to signal efficiency of ~80% and a coupling efficiency of the pump

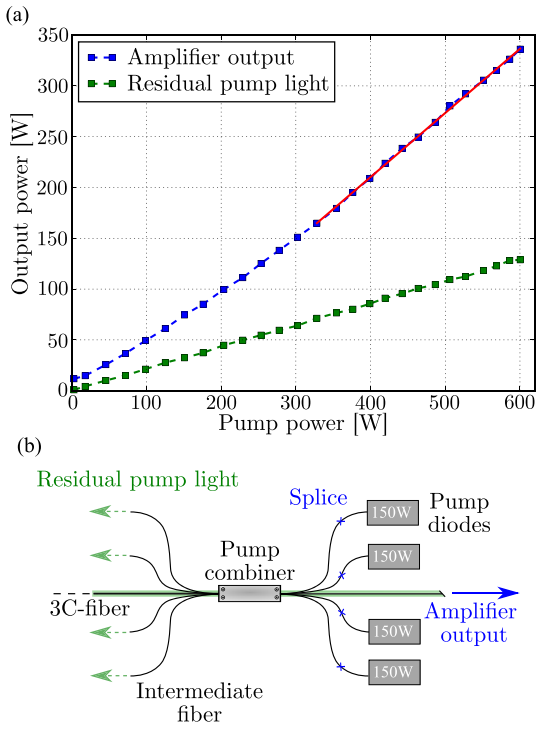

Fig. 4. (a) Slope of the amplifier with measured data (blue squares) and a linear fit (red line). The residual pump light of the pump combiner is shown in green. (b) Pump combiner integrated in the 3C-fiber with different fiber outputs for the non-transfered pump light.

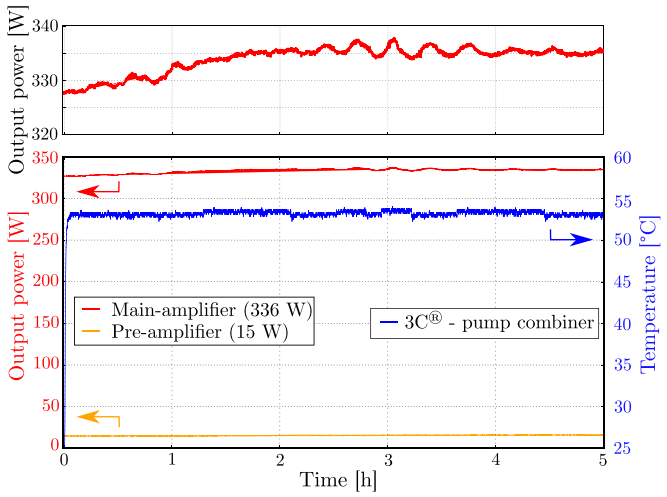

Fig. 5. Long-term power stability measurement of the 3C-fiber amplifier at an output power of 336 W in red and the corresponding pre-amplifier in orange. Additionally the behaviour of the output power at 336 W is shown in detail in the upper plot. The temperature of the high-power pump combiner integrated in the 3C-fiber is shown in blue.

combiner of ∼70%, the amplifier system reached a maximum output power of 336 W. As typically known from fiber amplifiers, the low efficiency at lower pump power levels was caused by the shifted center pump wavelength away from the absorption maximum of Yb^{3+} at 976 nm. A compensation at these power levels was only partially possible by an adjustment of the diode temperature. Due to the coupling efficiency of ∼70% of the pump combiner, a certain fraction of pump light could not be used in the amplification process. The amount of the residual pump light remaining in the intermediate fiber was ∼22% of the total diode power (see Fig. 4(a) and (b)). Accordingly, some residual pump light was lost in different ways in the pump combiner [17], which results in heating of the combiner housing. Therefore, the pump combiner was actively water-cooled for thermal management.

B. Power Stability in Operation

For a variety of applications, such as for GWDs, the reliability is essential in high-power operation. Therefore, the output power of the free-running amplifier system is shown in Fig. 5 in red in a continuous operation of the laser over 5 hours. The measurement includes a warm-up time of approximately 1 h, where the output power increases by 3.8% from 325 W to 336 W. In the curve (Fig. 5, upper plot), small fluctuations can be observed probably caused by temperature variations of the cooled, but not actively temperature stabilized aluminum fiber spool. Besides, the performance of the pre-amplifier of 15 W was monitored (Fig. 5, orange). In addition to the output power of the system, the temperature of the high-power pump combiner in the 3C-fiber was logged and is shown in Fig. 5 in blue. After a warm-up time, the housing of the combiner reached a constant temperature of $\sim 52 \pm 2\,^{\circ}\mathrm{C}$.

All in all, the 3C-fiber amplifier achieved an average output power during the operation test of (336.3 ± 2.7) W with a relative standard deviation of $<1\%$.

C. Optical Noise Characteristic

1) Spatial Beam Quality and Polarization Extinction Ratio: The application of GWDs can only utilize a pure TEM_{00}-mode and a linearly polarized beam in the interferometer, where a polarizing pre-mode cleaner cavity is integrated to suppress any higher order modes (HOMs). In general, for the characterisation of the beam quality of amplifier or laser systems, the M^2-measurement is a frequently used method. However, purely from the spatial information of the M^2-measurement, no statement can be made about the HOM-content of the beam. A low value of M^2 does not guarantee a pure single mode operation, as even an M^2 <1.1 can contain up to 30% of HOMs [22]. Thus, a meaningful characterization of the power in the fundamental mode is crucial to characterize laser sources for GWD and was done with a scanning ring-cavity as described by Kwee *et al.* in [23].

Fig. 2 shows a 3-mirror cavity in a non-confocal configuration as the measurement setup for the modal content, where the frequency of the eigenmodes of the ring-cavity changes by scanning the piezo attached to one of the mirrors over a free spectral range. Thereby, the beam was decomposed into a set of TEM_{ij} modes. The transmitted optical power of the corresponding modes was detected with a photodiode depending on a certain mirror position. For optimization of the mode matching into the cavity, a pair of lenses was installed in front of the setup. Because this technique requires low input power (<100 mW) in a linearly-polarized beam, the input power was adjusted by

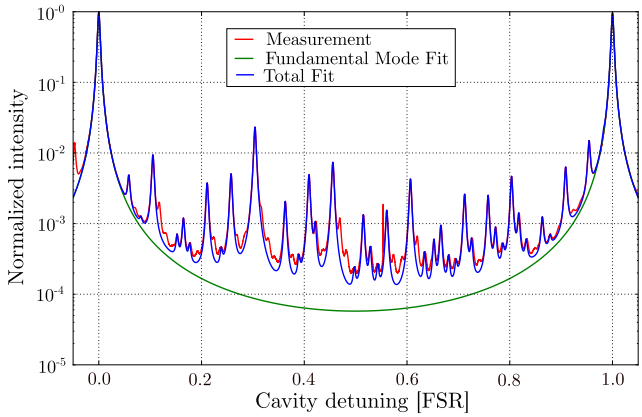

Fig. 6. Mode scan at an output power of 336 W with a fundamental mode content of 90.4%. The normalized intensity is shown in dependence of the cavity length over one free spectral range of the ring-cavity.

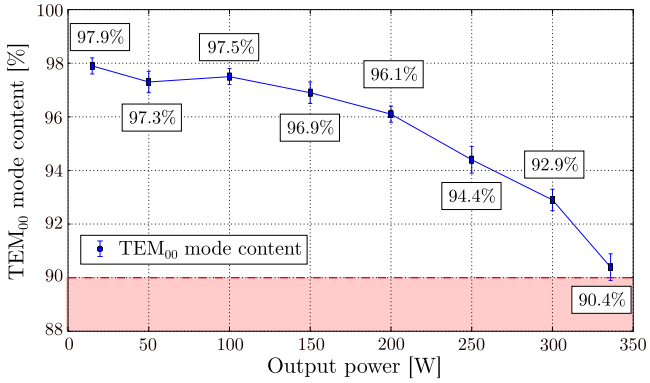

Fig. 7. TEM_{00}-mode content of 3C-fiber main-amplifier at different output power level. All measurements are above the requirements for GWDs of a TEM_{00} mode content of more than 90% [3].

a power tuning stage consisting of a half wave plate and a polarization beam splitter.

The normalized intensity in dependence of the cavity length over one free spectral range (FSR) of the cavity is presented in Fig. 6. Thereby, each data point was an average of 100 measurements to reduce effects of short time fluctuations. The averaged samples were used to fit functions of the fundamental Gaussian mode (green) and the total fit including a sum of fundamental and HOMs with variable coefficients (blue), where the ratio of the coefficients of these two fits determines the relative TEM_{00} mode content. By comparing the fits, inaccuracies in the measurement due to bad mode-matching to the cavity, potential amplified spontaneous emission (ASE) or residual unpolarized light could be minimized. At an output power level of 336 W the amplifier showed a modal content of 90.4% of the power in the fundamental mode.

At different output power levels, the corresponding TEM_{00} mode content was measured and is presented in Fig. 7. When only operating the pre-amplifier at a power level of ∼15 W (main amplifier stage off), a fundamental mode content of 97.9% was measured. Over the entire output power slope, the beam quality decreased to a TEM_{00} mode content of 90.4% at the maximum output power level of 336 W. To the best of our knowledge,

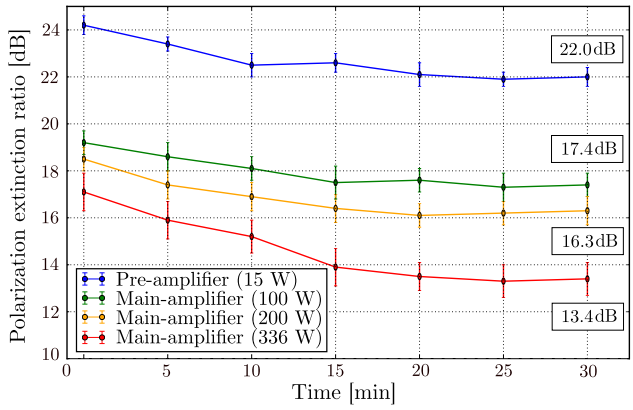

Fig. 8. Evolution of the polarization extinction ratio of 3C-fiber main-amplifier and the pre-amplifier at different output power levels over 30 minutes.

the fundamental mode content of 96.1% at 200 W exceeded the previous highest measured TEM_{00} mode content of 94.7% in conjunction with single-frequency lasers or amplifiers [9]. At all measurements of the evolution of the beam quality, the fundamental mode content was above the requirements (TEM_{00} mode content >90% [3]), which additionally emphasizes the high potential of fiber amplifiers based on 3C-fibers as laser sources for the next generation of GWDs. The observed slight decrease of the beam quality can be explained e.g. by the induced heat load and the impact on the modal loss reduction as reported by Zhu *et al.* [24].

In contrast to typical polarization-maintaining fibers, the design of the 3C-fiber has no further intrinsic birefringence due to additional stress cores. The preform of the 3C-fiber is rotated during the drawing process to achieve the helical design with rotating sidecores, which removes any residual intrinsic weak birefringence in the fiber [25]. Indeed, the polarization extinction ratio (PER) was only slightly affected as also previous measurements showed [7].

Fig. 8 shows the PER of a linearly polarized beam at different output power levels of the pre- and main-amplifier over a 30 minutes-measurement. Exclusively, the pre-amplifier exhibits a stable PER of (24.2±0.4) dB, which was reduced over the measurement duration to (22.0±0.4) dB. After the 3C-fiber of the main-amplifier the PER worsens at low main amplifier power to 17-19 dB due to the missing polarization-maintaining properties of the 3C-fiber. The orientation of the wave-plates was optimized on each output power level. At the maximum output power of 336 W the PER was reduced from (17.1±0.8) dB to a stable PER of (13.4±0.7) dB, which resulted in an additional power in an unusable polarization of approximately of 15 W. However, as long as the PER is stable over the long term, the additional losses are not critical and will not couple in power fluctuations after transmission through polarizing optical components or optical resonators.

Hence, taking into account the HOM content and the power in the wrong state of polarization, the overall output power in the linearly polarized TEM_{00}-mode was 289.9 W.

2) Relative Power Noise and Transverse Modal Instability Investigations: Laser sources for GWDs have to exhibit low

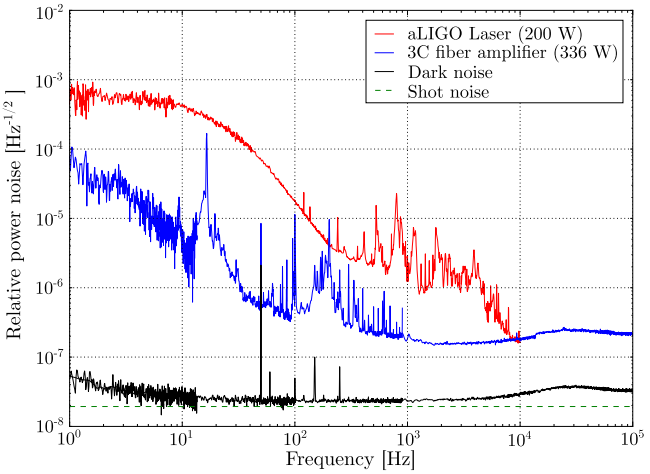

Fig. 9. Relative power noise measurements of the 3C-fiber amplifier system in comparison with the 200 W solid-state laser of the aLIGO detectors.

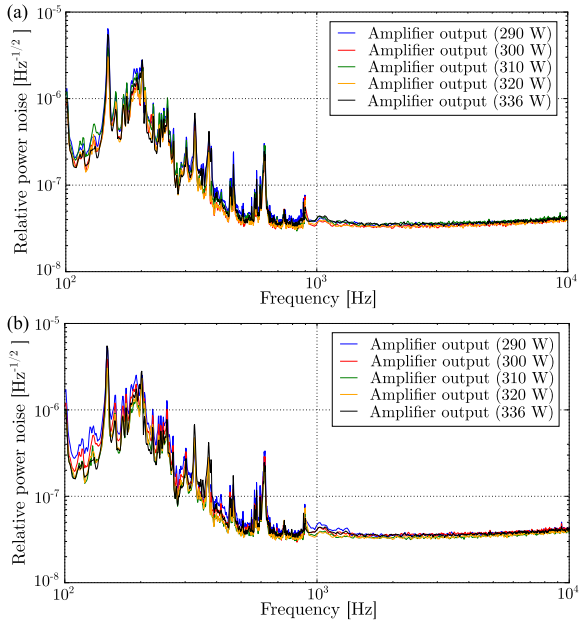

Fig. 10. (a) Relative power noise spectra at different output power levels without an aperture in the sampled beam. (b) Relative power noise spectra with an aperture in the sampled beam to convert modal fluctuations into power fluctuations.

power noise characteristics, because power fluctuations directly couple to the read-out signal of the detectors. Due to the fundamental frequencies of gravitational waves, the relative power noise (RPN) in the frequency range from 1 Hz to 100 kHz is relevant for the ground-based interferometers. Therefore, the RPN of the free-running laser system was analyzed up to a power level of 336 W. The utilized photodiode (PDA10CF, *Thorlabs*) was an InGaAs detector with 150 MHz bandwidth and the signal was analyzed with a SR785 (Stanford Research Systems) for FFT measurements. In Fig. 9, the RPN at the maximum power of the amplifier is compared to the measurements of the 200 W solid state laser-system developed for the aLIGO Hanford Observatory [29]. The presented fiber amplifier architecture with 3C-fibers exhibits a suitable RPN at all frequencies for the use in GWDs. Especially below 100 Hz, the measured RPN of the fiber amplifier is up to two orders of magnitudes lower compared to the RPN of GWD laser systems [1]. At higher frequencies above 10 kHz, the RPN of both systems achieve similar noise levels. The RPN in this frequency range is determined by the NPRO as seed source, which was used in both laser systems.

Thereby, the RPN characteristic was analyzed operated in a free-running laser system. The already very low RPN level of this 3C-fiber laser system can be further reduced by active power stabilization control schemes via e.g. pump power modulations as demonstrated by Thies *et al.* [2].

In the high-power regime, fiber amplifiers based on LMA fibers can exhibit effects of transverse modal instability (TMI). In recent years, TMI has come into the focus of research and has been extensively studied [31]. According to current knowledge, an induced thermal load and thermal gradient within fibers is the decisive physical parameter of the phenomenon of TMI. Jauregui *et al.* estimated a parameter of thermal load to the onset of TMI of around 34 W/m applicable to specific fiber geometries [32].

The presented results of the 3C-fiber amplifier regarding to the pump to signal efficiency of ∼80% in section III-A and the absolute efficiency are comparable to other fiber amplifier systems [9], [10]. With the estimated unabsorbed pump power of ∼20 W, additional pump light losses in the pump combiner housing of ∼8% and remaining pump light in the intermediate fibers of the pump combiner, the thermal load of the 3C-fiber was <33 W/m. Further signal losses due to the collimating lens and dichroic mirrors are not included. Thus, the thermal load of the 3C-fiber is below the introduced TMI limit.

Apparently, the HOM content of the laser system has a perceptible impact of onset of TMI [33]. Here, the 3C-fiber plays a special role, because it actively suppresses HOMs by its geometrical design and it should significantly increase the threshold of TMI. This influence of the 3C-fiber geometry on the TMI threshold opens a new research field for further investigations and could be interesting for a variety of such fiber-based applications. The behavior of the amplifier system with respect to TMI was experimentally investigated using the method described by Karow *et al.* [34]. The RPN was measured with and without an optical aperture in the beam path in front of the InGaAs photodiode in the frequency range of 100 Hz to 10 kHz. Due to the aperture, modal fluctuations are converted into power fluctuations. Above the TMI threshold, an excess RPN should be observable in discrete noise peaks in a 500 Hz-5 kHz frequency range or, far above the TMI threshold, in a broadband excess chaotic RPN. In Fig. 10 the RPN is presented in this frequency range with (a) and without (b) an aperture. Between both measurements there are no significant differences, neither discrete peaks nor a broadband excess RPN. The influence of the 3C-fiber design on the threshold of TMI at higher power levels is an interesting question and implies a high potential for following fiber amplifier systems.

3) Stimulated Brillouin Scattering Investigation: Single-frequency laser or amplifier systems are mainly limited by the onset of SBS [19]. The SBS threshold can be determined by

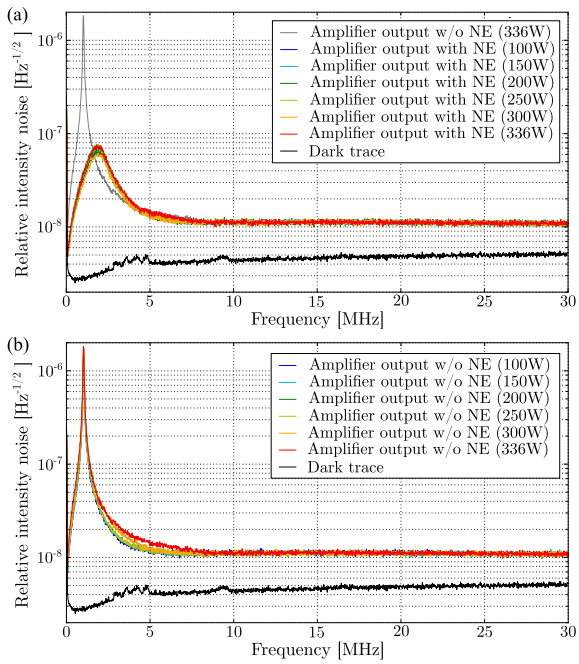

Fig. 11. Relative power noise spectra at different power levels up to a frequency range of 30 MHz. (a) With an additional integrated Noise Eater (NE) technology. (b) Without a NE. At 336 W a slight noise increase in the 5 MHz range can be detected.

several approaches, such as the common method of monitoring of backward propagating light or monitoring the relative power noise at high frequencies. Here, the effect is exploited that SBS imprints a broadband excess power noise in forward direction at MHz-frequencies [26]. This method is the most sensitive technique to determine the onset of SBS [19].

For application in GWDs, the MHz-regime is also relevant and cannot be neglected. In the interferometer this frequency range is used for length and alignment stabilizations. Here, modulation side bands are imprinted on the signal beam, which also require a low power noise at these frequencies [28]. Fig. 11 represents the relative power noise measured in the frequency range up to 30 MHz at different output power levels. The spectrum was detected with a spectrum analyzer E4440 A (*Agilent*) and the same photodiode as used in section III-C2. The intrinsic stability of the NPRO as seed source could be further improved by an additional integrated Noise Eater (NE) technology, which suppresses the relaxation oscillation peak of the NPRO. The differences in the Fourier spectrum using a NE or not are shown in Fig. 11(a) and (b). In b) the NE was switched off and the relative power noise is almost unchanged up to a power level of 300 W and then increases at 5 MHz slightly up to the maximum power of 336 W. This may indicate that the amplifier system showed the first onset of SBS at these power levels. However, this excess noise is typically more broadband and not limited locally to the 5 MHz range. According to Dixneuf *et al.* [10], the slightly increased intensity noise could be also attributed to the impact of residual cladding modes. This question can only be answered by future further power scaling experiments. In the spectrum in a) the NE was switched on. Here, the increase of the relative power noise is not clearly recognizable as in b) due to the slightly excess power noise in the frequency range of 2–3 MHz caused by the NE control loop of the NPRO. However, there is no impact of SBS recognizable in the slope in Fig. 4 and the amplifier system has no additional integrated techniques to suppress SBS yet. Thus, the SBS-threshold can be further increased by introducing a thermal gradient on the fiber to broaden the SBS gain spectrum [27]. In the experimental setup, this technique can be implemented by using two fiber spools at different temperatures. Indeed, the number of possible windings on two spools is limited by the fiber length and the required coiling diameter of 30 cm. Thus, a ratio of windings on two spools of maximum 1:2 can be practically achieved to generate a thermal gradient. The influence of this technique will have to be tested and can be integrated in a further improved engineering prototype of this 3C-fiber amplifier to achieve an even higher SBS-free output power.

IV. Conclusion

Chirally coupled core fibers emphasize the high potential for further power scaling of single-frequency fiber amplifiers. Such all-fiber amplifier systems are promising laser sources to fulfill the challenging requirements of GWDs. In this work, a compact and robust all-fiber architecture based on a special Yb^{3+}-doped 3C-fiber with a 34 μm core diameter has been demonstrated. For the first time, all optical components of the amplifier system were directly integrated in a single 3C-fiber to achieve a spliceless design and a high spatial purity. At an output power of 336 W, a fundamental mode content of 90.4% at a PER above 13 dB was demonstrated without an impact of TMI or other parasitic effects, however, with a first slight noise increase in the 5 MHz range which might indicate the first onset of SBS.

An integration of optical components in specialty fibers as 3C-fibers allows compact all-fiber systems, which can be implemented in almost any high-power amplifier or laser architectures. This work demonstrates the capability of such laser systems used in GWDs or in a variety of applications. Additionally, 3C-fibers with larger core diameter with single-mode guidance properties are under development and emphasize the high development potential of this innovative fiber type for further power scaling of all-(specialty) fiber amplifier or laser systems.

References

[1] L. Winkelmann *et al.*, "Injection-locked single-frequency laser with an output power of 220 W," *Appl. Phys. B*, vol. 102, no. 3, pp. 529–538, 2011.

[2] F. Thies, N. Bode, P. Oppermann, M. Frede, B. Schulz, and B. Willke, "Nd:YVO_4 high-power master oscillator power amplifier laser system for second-generation gravitational wave detectors," *Opt. Lett.*, vol. 44, pp. 719–722, 2018.

[3] ET Science Team, "Einstein gravitational wave telescope conceptual design study," ET-0106A-10, May 07, 2011. [Online]. Available: http://www.et-gw.eu/

[4] C. Basu, P. Weßels, J. Neumann, and D. Kracht, "High power single frequency solid state master oscillator power amplifier for gravitational wave detection," *Opt. Lett.*, vol. 37, pp. 2862–2864, 2012.

[5] M. Steinke *et al.*, "Single-frequency fiber amplifiers for next-generation gravitational wave detectors," *IEEE J. Sel. Topics Quantum Electron.*, vol. 24, no. 3, Jun. 2018, Art. no. 3100613.

[6] M. D. Mermelstein *et al.*, "All-fiber 194 W single-frequency single-mode Yb-doped master-oscillator power amplifier," in *Proc. SPIE*, vol. 6873, 2008, Art. no. 68730L.
[7] C. Zhu, I. Hu, X. Ma, and A. Galvanauskas, "Single-frequency and single-transverse mode Yb-doped CCC fiber MOPA with robust polarization SBS-free 511 W output," in *Proc. Adv. Opt. Mater., OSA Techn. Dig., Opt. Soc. Amer.*, 2011, Paper AMC5.
[8] B. Pulford, I. Dajani, and C. Robin, "Near diffraction-limited, 811 W, single-frequency photonic crystal fiber amplifier," in *Proc. Conf. Lasers Electro-Opt. (CLEO)-Laser Sci. Photon. Appl.*, 2014, pp. 1–2.
[9] F. Wellmann *et al.*, "High power, single-frequency, monolithic fiber amplifier for the next generation of gravitational wave detectors," *Opt. Express*, vol. 27, no. 20, pp. 28523–28533, 2019.
[10] C. Dixneuf *et al.*, "Ultra-low intensity noise, all fiber 365 w linearly polarized single frequency laser at 1064 nm," *Opt. Express*, vol. 28, pp. 10960–10969, 2020.
[11] G. Gu *et al.*, "Ytterbium-doped large-mode-area all-solid photonic bandgap fiber lasers," *Opt. Express*, vol. 22, 2014, Art. no. 13962.
[12] J. Limpert *et al.*, "Extended single-mode photonic crystal fiber lasers," *Opt. Express*, vol. 14, no. 7, pp. 2715–2720, 2006.
[13] C. Liu *et al.*, "Effectively single-mode chirally-coupled core fiber," *Adv. Solid-State Photon. OSA Tech. Dig. Ser.*, Paper ME2, 2007.
[14] X. Ma, C. Zhu, I-N. Hu, A. Kaplan, and A. Galvanauskas, "Single-mode chirally-coupled-core fibers with larger than 50 μm diameter cores," *Opt. Express*, vol. 22, pp. 9206–9219, 2014.
[15] S. Hochheim *et al.*, "Single-frequency chirally coupled-core all-fiber amplifier with 100 W in a linearly polarized TEM_{00} mode," *Opt. Lett.*, vol. 45, pp. 939–942, 2020.
[16] M. Wysmolek *et al.*, "Microstructured fiber cladding light stripper for kilowatt-class laser systems," *Appl. Opt.*, vol. 57, no. 23, pp. 6640–6644, 2018.
[17] T. Theeg, H. Sayinc, J. Neumann, L. Overmeyer, and D. Kracht, "Pump and signal combiner for bi-directional pumping of all-fiber lasers and amplifiers," *Opt. Express*, vol. 20, pp. 28125–28141, 2012.
[18] S. Hochheim *et al.*, "Highly-integrated signal and pump combiner in chirally-coupled-core fibers for all-fiber lasers and amplifiers," *J. Lightw. Technol.*, vol. 39, no. 22, pp. 7246–7250, Nov. 2021, doi: 10.1109/JLT.2021.3111993.
[19] M. Hildebrandt, S. Büsche, P. Weßels, M. Frede, and D. Kracht, "Brillouin scattering spectra in high-power single-frequency ytterbium doped fiber amplifiers," *Opt. Express*, vol. 16, no. 20, pp. 15970–15979, 2008.
[20] M. L. Stock, C.-H. Liu, A. Kuznetsov, G. Tudury, A. Galvanauskas, and T. Sosnowski, "Polarized, 100 kW peak power, high brightness nanosecond lasers based on 3 C optical fiber," *Fiber Lasers VIII: Technol., Syst., Appl., SPIE*, vol. 7914, pp. 170–178, 2011.
[21] C. Zhu *et al.*, "Chirally couple core (CCC) fiber lasers for coherent combining systems" Ph.D. dissertation, Univ. of Michigan, 2014.
[22] S. Wielandy, "Implications of higher-order mode content in large mode area fibers with good beam quality," *Opt. Express*, vol. 15, no. 23, pp. 15402–15409, 2007.
[23] P. Kwee, F. Seifert, B. Willke, and K. Danzmann, "Laser beam quality and pointing measurement with an optical resonator," *Rev. Sci. Instrum.*, vol. 78, no. 7, 2007, Art. no. 073103.
[24] S. Zhu *et al.*, "Impact of the heat load on the laser performance of chirally-coupled-core fibers," *Opt. Express*, vol. 27, no. 26, pp. 37522–37531, 2019.
[25] P. McIntyre and A. W. Snyder, "Light propagation in twisted anisotropic media: Application to photoreceptors," *J. Opt. Soc. Amer.*, vol. 68, no. 2, pp. 149–157, 1978.
[26] M. Horowitz, A. R. Chraplyvy, R. W. Tkach, and J. L. Zyskind, "Broadband transmitted intensity noise induced by stokes and anti-stokes Brillouin in single-mode fibers," *IEEE Photon. Technol. Lett.*, vol. 9, no. 1, pp. 124–126, Jan. 1997.
[27] A. Liu, X. Chen, M. J. Li, J. Wang, D. T. Walton, and L. A. Zenteno, "Comprehensive modeling of single frequency fiber amplifiers for mitigating stimulated brillouin scattering," *J. Lightw. Technol.*, vol. 27, no. 13, pp. 2189–2198, 2009.
[28] K. Izumi and D. Sigg, "Advanced LIGO: Length sensing and control in a dual recycled interferometric gravitational wave antenna," *Classical Quantum Gravity*, vol. 34, no. 1, 2017, Art. no. 015001.
[29] B. Willke *et al.*, "Pre-stabilized laser subsystem testing and acceptance - L1 PSL," Tech. Rep. No. LIGO-E1100716-v6, 2012.
[30] F. Thies, N. Bode, P. Oppermann, M. Frede, B. Schulz, and B. Willke, "Nd:YVO_4 high-power master oscillator power amplifier laser system for second-generation gravitational wave detectors," *Opt. Lett.*, vol. 44, no. 3, pp. 719–722, 2019.
[31] H.-J. Otto *et al.*, "Temporal dynamics of mode instabilities in high-power fiber lasers and amplifiers," *Opt. Express*, vol. 20, no. 14, 2012, Art. no. 15710.
[32] C. Jauregui, H.-J. Otto, F. Stutzki, J. Limpert, and A. Tünnermann, "Simplified modelling the mode instability threshold of high power fiber amplifiers in the presence of photodarkening," *Opt. Express*, vol. 23, no. 16, 2015, Art. no. 20203.
[33] M. M. Johansen, K. R. Hansen, M. Laurila, T. Tanggaard Alkeskjold, and J. Lægsgaard, "Estimating modal instability threshold for photonic crystal rod fiber amplifiers," *Opt. Express*, vol. 21, pp. 15409–15417, 2013.
[34] M. Karow, H. Tünnermann, J. Neumann, D. Kracht, and P. Weßels, "Beam quality degradation of a single-frequency Yb-doped photonic crystal fiber amplifier with low mode instability threshold power," *Opt. Lett.*, vol. 37, no. 20, 2012, Art. no. 4242.

Sven Hochheim was born in Gehrden, Germany, in 1991. He received the master's degree in physics from University Osnabrück, Osnabrück, Germany, in 2016. He is currently working toward the Ph.D. degree with the Cluster of Excellence Quantum Frontiers, Laser Zentrum Hannover e.V. (LZH), Hannover, Germany.

Eike Brockmüller biography not available at the time of publication.

Peter Wessels biography not available at the time of publication.

Joona Koponen biography not available at the time of publication.

Tyson Lowder biography not available at the time of publication.

Steffen Novotny biography not available at the time of publication.

Jörg Neumann biography not available at the time of publication.

Dietmar Kracht biography not available at the time of publication.